

Vorticity Preserving Schemes Using Potential-Based Fluxes for the System Wave Equation

Siddhartha Mishra and Eitan Tadmor

ABSTRACT. We consider the wave equation system in two-space dimensions. A new class of genuinely multi-dimensional finite volume schemes are designed, based on using vertex-centered numerical potentials. The resulting schemes preserve a discrete version of vorticity. Numerical experiments illustrating the robustness of the schemes are presented.

1. Introduction

We consider the linear wave equation in two dimensions,

$$(1.1) \quad p_{tt} - c^2 p_{xx} - c^2 p_{yy} = 0.$$

with constant speed c . By setting $u = p_x$ and $v = p_y$, the wave equation (1.1) can be written in the following first-order system form,

$$(1.2) \quad \begin{aligned} p_t + cu_x + cv_y &= 0, \\ u_t + cp_x &= 0, \\ v_t + cp_y &= 0. \end{aligned}$$

Note that the above system is a special case of a two-dimensional system of conservation laws of the form,

$$(1.3) \quad \mathbf{U}_t + (\mathbf{f}(\mathbf{U}))_x + (\mathbf{g}(\mathbf{U}))_y = 0, \quad (x, y, t) \in \mathbb{R} \times \mathbb{R} \times \mathbb{R}_+,$$

with the vector of unknowns denoted as $\mathbf{U} = \{p, u, v\}$ and the linear fluxes are given as $\mathbf{f}(\mathbf{U}) = A\mathbf{U}$ and $\mathbf{g}(\mathbf{U}) = B\mathbf{U}$, with matrices A, B given by

$$A = \begin{pmatrix} 0 & c & 0 \\ c & 0 & 0 \\ 0 & 0 & 0 \end{pmatrix}, \quad B = \begin{pmatrix} 0 & 0 & c \\ 0 & 0 & 0 \\ c & 0 & 0 \end{pmatrix}.$$

1991 *Mathematics Subject Classification.* 65M06,35L65.

Key words and phrases. system wave equation, vorticity, constraint transport, potentials.

Acknowledgment. The work on this paper was started when S.M. visited the Center of Scientific Computation and Mathematical Modeling (CSCAMM) and he thanks CSCAMM and all its members for the excellent hospitality and facilities. E. T. Research was supported in part by NSF grant 07-07949 and ONR grant N00014-09-1-0385.

A simple calculation shows that the eigenvalues of both A and B are $\Lambda = \{-c, 0, c\}$. Hence, the system (1.2) is strictly hyperbolic. It is also clearly symmetric.

We define the total energy of (1.2) as

$$E = \frac{1}{2}(p^2 + u^2 + v^2).$$

A simple calculation shows that smooth solutions of (1.2) satisfy the energy conservation property,

$$(1.4) \quad E_t + (cup)_x + (cvp)_y = 0.$$

This bound on energy provides an estimate in L^2 for the solutions of (1.2) and paves the way for establishing existence, uniqueness and stability of weak solutions of (1.2) by fairly standard arguments. In addition to energy preservation, another important invariant for (1.2) is the vorticity given by,

$$\omega = v_x - u_y.$$

Another simple calculation with (1.2) shows that

$$(1.5) \quad \omega_t \equiv 0.$$

Hence, the vorticity is preserved by the flow.

Our aim in this paper is to design suitable numerical schemes for simulating (1.2). An ideal numerical scheme for (1.2) should satisfy energy conservation (1.4) (at least for smooth solutions). Similarly, it should also preserve a discrete version of the vorticity ω . In addition, it should be easy to design and implement, accurate and robust.

The most popular schemes for simulating (possibly non-linear) conservation laws like (1.3) are the finite volume schemes (see [L] for a detailed description). In a finite volume approximation, the domain is discretized into cells or control volumes and an integral form of the conservation law (1.3) is approximated on each control volume. The resulting method relies on updating cell averages of the unknown over each control volume by the construction of suitable numerical fluxes across each cell interface. To illustrate this method, we consider a uniform Cartesian discretization of the domain with mesh sizes Δx and Δy in the x - and y - directions respectively. Denoting $x_i = i\Delta x$ and $y_j = j\Delta y$, a typical Cartesian cell is denoted as $I_{i,j} = [x_{i-1/2}, x_{i+1/2}] \times [y_{j-1/2}, y_{j+1/2}]$ and the cell average of \mathbf{U} over $I_{i,j}$ at time t is denoted as $\mathbf{U}_{i,j}(t)$. Then, a typical finite volume scheme for (1.3) (see [L]) takes the form,

$$(1.6) \quad \frac{d}{dt} \mathbf{U}_{i,j} = \delta_x \mathbf{F}_{i,j} + \delta_y \mathbf{G}_{i,j}$$

Here, δ_x, δ_y denote the standard centered differences,

$$(1.7) \quad \delta_x \mathbf{F}_{i,j} := \frac{1}{\Delta x} \left(\mathbf{F}_{i+\frac{1}{2},j} - \mathbf{F}_{i-\frac{1}{2},j} \right), \quad \delta_y \mathbf{G}_{i,j} := \frac{1}{\Delta y} \left(\mathbf{G}_{i,j+\frac{1}{2}} - \mathbf{G}_{i,j-\frac{1}{2}} \right)$$

where $\mathbf{F}_{i+\frac{1}{2},j} = \mathbf{F}(\dots, \mathbf{U}_{i,j}, \mathbf{U}_{i+1,j}, \dots)$ and $\mathbf{G}_{i,j+\frac{1}{2}} = \mathbf{G}(\dots, \mathbf{U}_{i,j}, \mathbf{U}_{i,j+1}, \dots)$ are any numerical fluxes in the x - and y -directions which are consistent with the differential fluxes \mathbf{f}, \mathbf{g} . For notational convenience, we have suppressed the time dependence of all the quantities.

We would like to point out that finite volume scheme (1.6) is based on using one dimensional fluxes \mathbf{F}, \mathbf{G} across the cell interface in each normal direction. Despite the tremendous success of finite volume schemes (1.6), they are known to be

deficient when it comes to resolving genuinely multi-dimensional behavior of the solutions of (1.3) ([L]). This is to be expected as the schemes are based on local one-dimensional fluxes in each direction and don't incorporate any genuinely multi-dimensional information, thus leading to instabilities and poor resolution when applied to multi-dimensional conservation laws. The same deficiencies are observed when one uses a finite volume scheme like (1.6) to the wave equation (1.2) with the resulting scheme being unable to resolve multi-dimensional waves in a robust manner.

Furthermore, a finite volume scheme like (1.6) will not necessarily preserve any discrete version of the vorticity. This leads to a loss of accuracy on problems where vorticity preservation is important. The lack of vorticity preservation at the level of the scheme is a consequence of the fact the scheme (1.6) is not genuinely multi-dimensional (GMD) whereas the vorticity preservation (1.5) is a direct manifestation of multi-dimensional effects in (1.2). Hence, this model has been suggested ([MR],[LMW]) as a prototype for the design of genuinely multi-dimensional schemes for systems of conservation laws in a manner similar to the use of linear advection equation as a toy model to design highly efficient numerical schemes for conservation laws in one space dimension.

Many other hyperbolic problems also involve constraints. Examples include the equations of magneto-hydrodynamics (MHD) where the divergence of the magnetic field is preserved by the flow. The design of numerical schemes for conservation laws with constraints is a very active area of research and many different methods have been suggested. A good review of methods to preserve divergence in MHD equations is provided in [T]. Vorticity preservation for the system wave equation (1.2) has been studied in [MR] and [JT].

We propose a different approach to designing genuinely multi-dimensional finite volume schemes for systems of conservation laws (1.3). The framework consists of re-writing the edge-centered numerical fluxes \mathbf{F} , \mathbf{G} in terms of vertex centered potentials. The potentials are chosen such that the resulting scheme will be consistent. In addition, the potentials incorporate transverse information into the scheme. This approach leads to a simple, easy to implement, computationally inexpensive and stable approach for designing GMD schemes. Simple modifications of the potentials lead to preservation of interesting constraints. We have described this new approach in the context of the magnetic induction equations (where divergence is preserved) in [MT1], the Euler equations of gas dynamics in [MT2] and the equations of MHD in [MT3]. We will illustrate this approach for the system wave equation in this paper. We present potential based finite volume schemes preserving vorticity. Some examples of these scheme also preserve energy. The performance of these schemes is illustrated on a set of numerical experiments.

2. Potential based GMD schemes

We begin with the description of the potential-based schemes presented in [MT2]. We let $\mathbf{F}_{i+\frac{1}{2},j}$, $\mathbf{G}_{i,j+\frac{1}{2}}$ be any two finite volume fluxes in the x - and y -directions which could be expressed as averages of vector numerical potentials Φ and Ψ ,

$$(2.1) \quad \mathbf{F}_{i+\frac{1}{2},j} = \mu_y \Phi_{i+\frac{1}{2},j}, \quad \mathbf{G}_{i,j+\frac{1}{2}} = \mu_x \Psi_{i,j+\frac{1}{2}}.$$

Here, μ_x, μ_y denote the usual averaging operators in the x - and y -directions, respectively,

$$(2.2) \quad \mu_y \Phi_{i+\frac{1}{2},j} = \frac{1}{2} \left(\Phi_{i+\frac{1}{2},j+\frac{1}{2}} + \Phi_{i+\frac{1}{2},j-\frac{1}{2}} \right), \quad \mu_x \Phi_{i,j+\frac{1}{2}} = \frac{1}{2} \left(\Phi_{i+\frac{1}{2},j+\frac{1}{2}} + \Phi_{i-\frac{1}{2},j+\frac{1}{2}} \right),$$

where $\Phi_{i+\frac{1}{2},j+\frac{1}{2}} = \Phi(\dots, \mathbf{U}_{i,j}, \mathbf{U}_{i+1,j+1}, \dots)$ and $\Psi_{i+\frac{1}{2},j+\frac{1}{2}} = \Psi(\dots, \mathbf{U}_{i,j}, \mathbf{U}_{i+1,j+1}, \dots)$ are arbitrary vector potentials with the sole requirement that they need to be consistent, i.e., $\Phi_{i+\frac{1}{2},j+\frac{1}{2}}(\mathbf{u}, \dots, \mathbf{u}) = \mathbf{f}(\mathbf{u})$ and $\Psi_{i+\frac{1}{2},j+\frac{1}{2}}(\mathbf{u}, \dots, \mathbf{u}) = \mathbf{g}(\mathbf{u})$. Observe that fluxes centered in the x - and y -edges of the computational cells are sought to be expressed as averages of vector numerical potentials in the normal directions. Examples of such potentials will be specified later.

The (semi-discrete) potential-based finite-volume scheme (1.6),(2.1) now reads

$$(2.3) \quad \frac{d}{dt} \mathbf{U}_{i,j} = -\delta_x \mu_y \Phi_{i,j} - \delta_y \mu_x \Psi_{i,j}.$$

The above scheme is clearly conservative. Since the potentials are assumed to be consistent, the above scheme is also consistent approximation of (1.3). A glimpse of the genuinely multi-dimensional nature of the scheme is already evident in the form (2.3) as the potentials are differenced in the normal direction but averaged in the transverse direction. The structure will be more explicit once we specify the form the potentials Φ, Ψ .

The framework of potential-based schemes applies to general multidimensional problems [MT1, MT2, MT3]. We turn our attention to the specific case of wave system (1.2) which preserves a discrete form of vorticity. Hence, we need to choose the potentials

$$(2.4a) \quad \Phi = (\Phi^1 = \phi, \Phi^2 = \eta, \Phi^3 = 0)^\top, \quad \Psi = (\Psi^1 = \psi, \Psi^2 = 0, \Psi^3 = \eta)^\top.$$

Observe that $\Phi^3 = \Psi^2 = 0$ are made consistent with $\mathbf{f}^3 = \mathbf{g}^2 = 0$. Next, (1.2) requires $\Phi^2 = \Psi^3$ should be consistent with $\mathbf{f}^2 = \mathbf{g}^3 \equiv cp$, hence, we choose $\phi^2 = \psi^3 = \eta$ where η is a scalar potential satisfying

$$(2.4b) \quad \eta(\mathbf{U}, \mathbf{U}, \dots, \mathbf{U}) = cp.$$

Finally, we have the freedom to choose scalar potentials ϕ, ψ which satisfy the consistency conditions,

$$(2.4c) \quad \phi(\mathbf{U}, \mathbf{U}, \dots, \mathbf{U}) = cu, \quad \psi(\mathbf{U}, \mathbf{U}, \dots, \mathbf{U}) = cv.$$

We rewrite the potential-based scheme (2.3),(2.4) for the system wave equation (1.2) with the above potentials, obtaining the following class of semi-discrete finite volume schemes,

$$(2.5) \quad \begin{aligned} \frac{d}{dt} p_{i,j} &= -\delta_x \mu_y \phi_{i,j} - \delta_y \mu_x \psi_{i,j}, \\ \frac{d}{dt} u_{i,j} &= -\delta_x \mu_y \eta_{i,j}, \\ \frac{d}{dt} v_{i,j} &= -\delta_y \mu_x \eta_{i,j}. \end{aligned}$$

We end up with a class of schemes, (2.5), which are clearly consistent and conservative. Moreover, this class of potential-based schemes preserve the following discrete

vorticity operator,

$$\begin{aligned}
 \omega_{i,j}^* &= \mu_y \delta_x v_{i,j} - \mu_x \delta_y u_{i,j} \\
 (2.6) \quad &\equiv \frac{1}{8\Delta x} ((v_{i+1,j+1} + 2v_{i+1,j} + v_{i+1,j-1}) - (v_{i-1,j+1} + 2v_{i-1,j} + v_{i-1,j-1})) \\
 &\quad - \frac{1}{8\Delta y} ((u_{i+1,j+1} + 2u_{i,j+1} + u_{i-1,j+1}) - (u_{i+1,j-1} + 2u_{i,j-1} + u_{i-1,j-1})).
 \end{aligned}$$

This is the content of the following lemma.

LEMMA 2.1. *Let $u_{i,j}, v_{i,j}$ be numerical solutions given by the scheme (2.5). Let the discrete vorticity ω^+ be given by (2.6), then we have*

$$\frac{d}{dt} \omega_{i,j}^* \equiv 0, \quad \forall i, j.$$

PROOF. We observe that the difference operators δ_x, δ_y and the averaging operators μ_x, μ_y commute with each other. Applying the discrete vorticity operator ω^* to the numerical scheme (2.5), we arrive at the following form,

$$\frac{d}{dt} \omega_{i,j}^* + (\mu_y \delta_x \delta_y \mu_x - \mu_x \delta_y \delta_x \mu_y) \eta_{i,j} = 0.$$

Commutativity of the averaging and difference operators implies that

$$\mu_x \delta_y \delta_x \mu_y \equiv \mu_y \delta_x \delta_y \mu_x,$$

which implies that

$$\frac{d}{dt} \omega_{i,j}^* \equiv 0.$$

□

Thus choosing any consistent potential in (2.5) leads to a numerical scheme that preserves the discrete vorticity (2.6).

2.1. Specifying numerical potentials. The scheme (2.5) with any consistent choice of potential preserves vorticity. There are many possible choices of potentials leading to robust results. Let \mathbf{F}, \mathbf{G} be *any* two standard finite volume fluxes consistent with the fluxes \mathbf{f}, \mathbf{g} in (1.2),(1.3). We can choose potentials in the following manner,

(1) : (*Symmetric potential*):

$$\begin{aligned}
 \phi_{i+\frac{1}{2},j+\frac{1}{2}} &= \frac{1}{2} (\mathbf{F}^1(\mathbf{U}_{i,j}, \mathbf{U}_{i+1,j}) + \mathbf{F}^1(\mathbf{U}_{i,j+1}, \mathbf{U}_{i+1,j+1})), \\
 \psi_{i+\frac{1}{2},j+\frac{1}{2}} &= \frac{1}{2} (\mathbf{G}^1(\mathbf{U}_{i,j}, \mathbf{U}_{i,j+1}) + \mathbf{G}^1(\mathbf{U}_{i+1,j}, \mathbf{U}_{i+1,j+1})), \\
 \eta_{i+\frac{1}{2},j+\frac{1}{2}} &= \frac{1}{4} (\mathbf{F}^2(\mathbf{U}_{i,j}, \mathbf{U}_{i+1,j}) + \mathbf{F}^2(\mathbf{U}_{i,j+1}, \mathbf{U}_{i+1,j+1}) \\
 &\quad + \mathbf{G}^3(\mathbf{U}_{i,j}, \mathbf{U}_{i,j+1}) + \mathbf{G}^3(\mathbf{U}_{i+1,j}, \mathbf{U}_{i+1,j+1})).
 \end{aligned}
 \tag{2.7}$$

Clearly, the above choice of potential is consistent. Furthermore, the above potential is obtained by averaging edge-centered fluxes in the transverse direction.

(2) (*Diagonal Potential:*)

$$(2.8) \quad \begin{aligned} \phi_{i+\frac{1}{2},j+\frac{1}{2}} &= \frac{1}{2}(\mathbf{F}^1(\mathbf{U}_{i,j}, \mathbf{U}_{i+1,j+1}) + \mathbf{F}^1(\mathbf{U}_{i,j+1}, \mathbf{U}_{i+1,j})), \\ \psi_{i+\frac{1}{2},j+\frac{1}{2}} &= \frac{1}{2}(\mathbf{G}^1(\mathbf{U}_{i,j}, \mathbf{U}_{i+1,j+1}) + \mathbf{G}^1(\mathbf{U}_{i+1,j}, \mathbf{U}_{i,j+1})), \\ \eta_{i+\frac{1}{2},j+\frac{1}{2}} &= \frac{1}{4}(\mathbf{F}^2(\mathbf{U}_{i,j}, \mathbf{U}_{i+1,j+1}) + \mathbf{F}^2(\mathbf{U}_{i,j+1}, \mathbf{U}_{i+1,j}) \\ &\quad + \mathbf{G}^3(\mathbf{U}_{i,j}, \mathbf{U}_{i+1,j+1}) + \mathbf{G}^3(\mathbf{U}_{i+1,j}, \mathbf{U}_{i,j+1})). \end{aligned}$$

The above choice of potential is also consistent. Note that it introduces a new type of flux obtained by considering states along the diagonal. This choice of potential in a slightly different context was introduced in [MT1, MT3].

We will test both potentials in our numerical experiments. In-order to specify the scheme completely, we need to choose some suitable numerical fluxes \mathbf{F} , \mathbf{G} used in the definition (2.7),(2.8). We start with the following choice.

2.1.1. *Central flux:* We choose the following numerical flux,

$$(2.9) \quad \mathbf{F}(\mathbf{U}_{i,j}, \mathbf{U}_{i+1,j}) = \frac{1}{2}(\mathbf{f}(\mathbf{U}_{i,j}) + \mathbf{f}(\mathbf{U}_{i+1,j})), \quad \mathbf{G}(\mathbf{U}_{i,j}, \mathbf{U}_{i,j+1}) = \frac{1}{2}(\mathbf{g}(\mathbf{U}_{i,j}) + \mathbf{g}(\mathbf{U}_{i,j+1})),$$

This is the standard central flux for finite volume schemes. Using (2.9) in both the symmetric potential ((2.7)) and the diagonal potential ((2.8)) results in exactly the same form of the scheme (2.5). The scheme takes the explicit form,

$$(2.10) \quad \begin{aligned} \frac{d}{dt} p_{i,j} &= -\frac{c}{8\Delta x}(u_{i+1,j+1} + 2u_{i+1,j} + u_{i+1,j-1}) + \frac{c}{8\Delta x}(u_{i-1,j+1} + 2u_{i-1,j} + u_{i-1,j-1}) \\ &\quad - \frac{c}{8\Delta y}(v_{i+1,j+1} + 2v_{i,j+1} + v_{i-1,j+1}) + \frac{c}{8\Delta y}(v_{i+1,j-1} + 2v_{i,j-1} + v_{i-1,j-1}), \\ \frac{d}{dt} u_{i,j} &= -\frac{c}{8\Delta x}(p_{i+1,j+1} + 2p_{i+1,j} + p_{i+1,j-1}) + \frac{c}{8\Delta x}(p_{i-1,j+1} + 2p_{i-1,j} + p_{i-1,j-1}), \\ \frac{d}{dt} v_{i,j} &= -\frac{c}{8\Delta y}(p_{i+1,j+1} + 2p_{i,j+1} + p_{i-1,j+1}) + \frac{c}{8\Delta y}(p_{i+1,j-1} + 2p_{i,j-1} + p_{i-1,j-1}). \end{aligned}$$

The above scheme is second-order accurate. In addition it also satisfies the following discrete energy preservation identity,

$$(2.11) \quad \frac{d}{dt} \sum_{i,j} E_{i,j} \equiv 0,$$

where discrete energy $E_{i,j}$ is the discrete equivalent of energy. The proof of the above energy identity is rather straightforward and we omit it due to constraints of space. Note that the second-order scheme (2.10) is unstable with respect to forward Euler time stepping and we need to use a suitable strong-stability preserving Runge-Kutta time stepping for time integration. Furthermore, this scheme preserves energy and will generate oscillations near discontinuities. Hence, we add some numerical diffusion to obtain non-oscillatory approximation of discontinuous solutions.

2.1.2. *Rusanov flux*: A simple way of adding numerical diffusion to (2.10) is to use the Rusanov flux of the form,

$$(2.12) \quad \begin{aligned} \mathbf{F}(\mathbf{U}_{i,j}, \mathbf{U}_{i+1,j}) &= \frac{1}{2}(\mathbf{f}(\mathbf{U}_{i,j}) + \mathbf{f}(\mathbf{U}_{i+1,j}) - |c|(\mathbf{U}_{i+1,j} - \mathbf{U}_{i,j})), \\ \mathbf{G}(\mathbf{U}_{i,j}, \mathbf{U}_{i,j+1}) &= \frac{1}{2}(\mathbf{g}(\mathbf{U}_{i,j}) + \mathbf{g}(\mathbf{U}_{i,j+1}) - |c|(\mathbf{U}_{i,j+1} - \mathbf{U}_{i,j})). \end{aligned}$$

In this simple case of constant velocity, the Rusanov flux coincides with the standard upwind flux. We substitute this value of the Rusanov flux in the expressions of the symmetric potential (2.7) and diagonal potential (2.8) and obtain two different forms of the vorticity-preserving scheme (2.5). Hence, the difference between the two potentials lies in the explicit form of the numerical diffusion. We omit the explicit expressions of the schemes due to limited space.

Both resulting schemes are limited to first order accuracy in space. We can easily obtain second-order accuracy by using non-oscillatory piecewise polynomials employing suitable slope limiters. We follow the second-order reconstruction procedure of Kurganov-Tadmor ([**KT**]).

3. Numerical Experiments

In this section, we will test the potential based vorticity preserving GMD schemes (2.5) on a set of numerical experiments. We consider four different form of (2.5): the second-order accurate central scheme (2.10) with second-order Runge-Kutta time stepping, (2.5) with first-order symmetric-potential (2.7) and forward Euler time stepping, (2.5) with first-order diagonal potential (2.8) and forward Euler time stepping and (2.5) with second-order diagonal potential (2.8) and second-order Runge-Kutta time stepping. The schemes will be denoted as GMDcen, GMDsym, GMDdiag and GMDdiaghr respectively. All the schemes are updated in time with a CFL number of 0.9.

3.1. Numerical Experiment 1: (Smooth solutions). This numerical experiment was considered in [**LMW**] and considers the system wave equation (1.2) in the domain $[-2, 2] \times [-2, 2]$ with the initial data,

$$(3.1) \quad \begin{aligned} p(x, y, 0) &= -ce^{-15(x^2+y^2)}, \\ u(x, y, 0) &= v(x, y, 0) \equiv 0, \end{aligned}$$

with $c = 1$. The initial data is smooth and the exact solution consists of a smooth circular wave propagating outwards. We compute the approximate solution with all the four schemes mentioned above on a uniform 200×200 mesh and plot the variable p at time $t = 0.5$ in figure 1. The results in figure 1 show that all the GMD schemes do very well in approximating the circular waves. The two first-order schemes resolve the solution without any noticeable difference. The first-order schemes are more diffusive than the second-order schemes. Another measure of the numerical performance are vorticity errors. We start with zero initial vorticity and the vorticity should remain zero in time. We compute the discrete vorticity (2.6) and show the L^1 norm of the vorticity at time $t = 0.5$ in table 1. The table show that all the GMD schemes preserve the discrete vorticity and the vorticity errors are very low, at a magnitude comparable to machine precision.

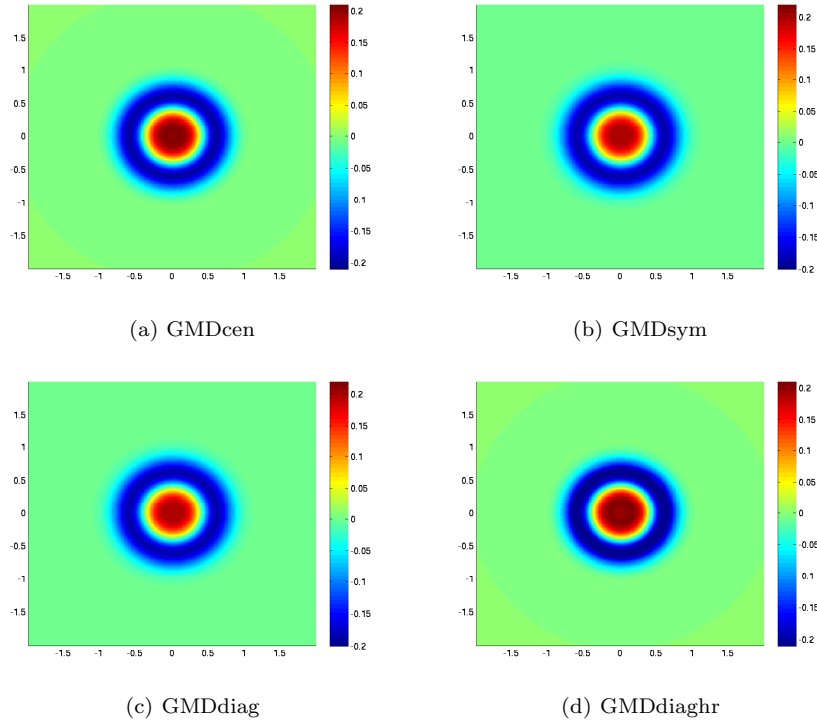


FIGURE 1. Approximate solutions of p for numerical experiment 1 at $t = 0.5$ on a 200×200 mesh computed with first order GMDsym, GMDdiag and second order GMDcen, GMDdiaghr schemes.

M	GMDsym	GMDdiag	GMDdiaghr	GMDcen
50	9.3e-11	1.5e-12	3.5e-16	6.7e-16
100	2.8e-14	8.5e-15	1.3e-16	2.4e-16
200	7.9e-16	9.4e-16	1.3e-17	9.5e-17
400	2.1e-17	3.0e-17	4.5e-18	1.6e-17

TABLE 1. Vorticity errors in L^1 for numerical experiment 1.

3.2. Numerical experiment 2 (Discontinuous solutions): We conclude the discussion on the system wave equation by consider the following discontinuous initial data as [LMW],

$$(3.2) \quad p(x, y, 0) = \begin{cases} 1 & \text{if } \sqrt{x^2 + y^2} \leq 0.4 \\ 0 & \text{otherwise,} \end{cases}$$

$$u(x, y, 0) = v(x, y, 0) \equiv 0.$$

The aim of this experiment is to test how the outer propagating circular shock is resolved by the GMD schemes and how the discrete vorticity is handled by them. The numerical results for p for a uniform 200×200 mesh on the domain $[-2, 2] \times [-2, 2]$ at time $t = 0.5$ for all the four schemes is shown in figure 2. As

expected, the two first schemes are diffusive but resolve the outer circular quite well. The second-order GMDdiaghr scheme is very robust and captures the shock with little smearing. The GMDcen scheme is a central schemes and is oscillatory near the shock. The vorticity errors generated by the schemes are shown in table 2 and illustrate that all the schemes preserve discrete vorticity.

M	GMDsym	GMDdiag	GMDdiaghr	GMDcen
50	3.99e-12	8.11e-13	1.5e-16	2.1e-16
100	1.73e-15	3.9e-15	0.4e-16	6.6e-17
200	1.4e-16	1.6e-16	1.9e-17	3.5e-17
400	3.8e-17	8.0e-17	0.5e-17	0.6e-17

TABLE 2. Vorticity errors in L^1 for numerical experiment 2.

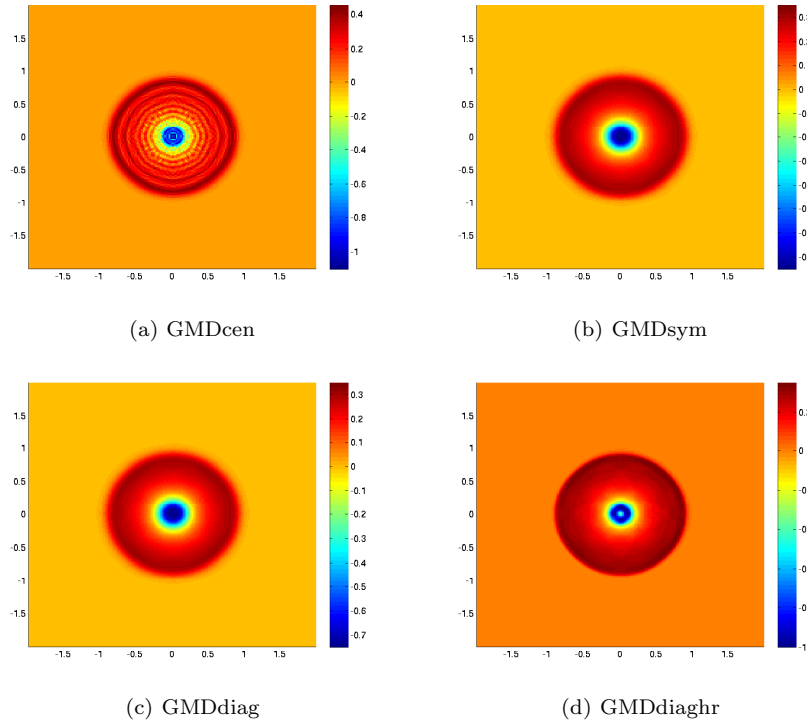


FIGURE 2. Approximate solutions of p for numerical experiment 2 at $t = 0.5$ on a 200×200 mesh computed with first order GMDsym, GMDdiag and second order GMDcen, GMDdiaghr schemes.

To summarize, we design genuinely multi-dimensional finite volume schemes for the system wave equation (1.2). The schemes are based on introducing vertex-centered potentials. The form of potentials enables incorporation of transverse information. The resulting schemes are GMD. Suitable choices of potentials leads to schemes that preserve a discrete version of vorticity. Using a standard central flux in

defining potentials leads to a scheme that preserves both vorticity and total energy. Numerical experiments illustrating the robustness of the schemes in resolving multi-dimensional waves are presented. This new approach based on potentials is very promising in dealing with the simulation of conservation laws in multi-dimensions, particularly problems with constraints. Further results on this approach can be found in [MT1, MT2, MT3].

References

- [JT] R. Jeltsch and M. Torrilhon. On curl preserving finite volume discretizations of the shallow water equations. *BIT*, 46, 2006, suppl.
- [KT] A. Kurganov and E. Tadmor. New high resolution central schemes for non-linear conservation laws and convection-diffusion equations. *J. Comput. Phys*, 160(1), 241-282, 2000.
- [L] R. J. LeVeque. Finite volume methods for hyperbolic problems. *Cambridge university press*, Cambridge, 2002.
- [LMW] M. Lukacova-Medvidova, K. W. Morton and G. Warnecke. Evolution Galerkin methods for Hyperbolic systems in two space dimensions. *Math. Comp.*, 69 (232), 1355 - 1384, 2000.
- [MT1] S. Mishra and E. Tadmor. Constraint preserving schemes using potential-based fluxes I: Multi-dimensional transport equations. *Preprint*, 2008.
- [MT2] S. Mishra and E. Tadmor. Constraint preserving schemes using potential-based fluxes I: Genuinely multi-dimensional central schemes for systems of conservation laws. *Preprint*, 2008.
- [MT3] S. Mishra and E. Tadmor. Constraint preserving schemes using potential-based fluxes III: Genuinely multi-dimensional central schemes for MHD equations. *Preprint*, 2008.
- [MR] K. W. Morton and P. L. Roe. Vorticity preserving Lax-Wendroff type schemes for the system wave equation. *SIAM. J. Sci. Comput.*, 23 (1), 2001, 170-192.
- [T] G. Toth. The $\text{Div}B = 0$ constraint in shock capturing magnetohydrodynamics codes. *J. Comp. Phys.*, 161:605-652, 2000.

(Siddhartha Mishra)

CENTRE OF MATHEMATICS FOR APPLICATIONS (CMA)
 UNIVERSITY OF OSLO
 P.O. BOX 1053, BLINDERN
 N-0316 OSLO, NORWAY
E-mail address: `siddharm@cma.uio.no`

(Eitan Tadmor)

DEPARTMENT OF MATHEMATICS
 CENTER OF SCIENTIFIC COMPUTATION AND MATHEMATICAL MODELING (CSCAMM)
 INSTITUTE FOR PHYSICAL SCIENCES AND TECHNOLOGY (IPST)
 UNIVERSITY OF MARYLAND
 MD 20741-4015, USA
E-mail address: `tadmor@cscamm.umd.edu`